



TITLE:

# Brilliant gamma beams for industrial applications: new opportunities, new challenges

AUTHOR(S):

Iancu, V; Suliman, G; Turturica, G V; Iovea, M; Daito, I; Ohgaki, H; Matei, C; Ur, C A; Balabanski, D L

---

CITATION:

Iancu, V ...[et al]. Brilliant gamma beams for industrial applications: new opportunities, new challenges. Journal of Physics: Conference Series 2016, 763: 012003.

ISSUE DATE:

2016-10

URL:

<http://hdl.handle.net/2433/219648>

RIGHT:

Content from this work may be used under the terms of the Creative Commons Attribution 3.0 licence. Any further distribution of this work must maintain attribution to the author(s) and the title of the work, journal citation and DOI.

## Brilliant gamma beams for industrial applications: new opportunities, new challenges

This content has been downloaded from IOPscience. Please scroll down to see the full text.

2016 J. Phys.: Conf. Ser. 763 012003

(<http://iopscience.iop.org/1742-6596/763/1/012003>)

View [the table of contents for this issue](#), or go to the [journal homepage](#) for more

Download details:

IP Address: 130.54.110.32

This content was downloaded on 20/04/2017 at 02:21

Please note that [terms and conditions apply](#).

You may also be interested in:

[Future Experiments with Intense Laser Beams and Brilliant Gamma Beams at the ELI-NP Facility](#)

Dimiter L Balabanski and the ELI-NP Science Team

[Status of the project for a positron laboratory at ELI-NP](#)

N Djourellov, A Oprisa, D Dinescu et al.

[Improving Reliability of Service Operation Using FMEA Review and New Opportunity for Investigations](#)

Agung Sutrisno and Indra Gunawan

[The BGO Calorimeter of BGO-OD Experiment](#)

B Bantes, D Bayadilov, R Beck et al.

[New frontiers in nuclear physics with high-power lasers and brilliant monochromatic gamma beams](#)

S Gales, D L Balabanski, F Negoita et al.

[Helium burning: Carbon and oxygen formation studied with an optical readout TPC \(O-TPC\)](#)

Moshe Gai and the Uconn-Yale-Duke-Weizmann-Ptb-Ucl collaboration

[Monte Carlo calculated output factors of a Leksell Gamma Knife unit](#)

Joel Y C Cheung, K N Yu, Robert T K Ho et al.

# Brilliant gamma beams for industrial applications: new opportunities, new challenges

V Iancu<sup>1</sup>, G Suliman<sup>1</sup>, G V Turturica<sup>1</sup>, M Iovea<sup>2</sup>, I Daito<sup>3</sup>, H Ohgaki<sup>3</sup>, C Matei<sup>1</sup>, C A Ur<sup>1</sup> and D L Balabanski<sup>1</sup>

<sup>1</sup> Extreme Light Infrastructure-Nuclear Physics/ Horia Hulubei National Institute for R&D in Physics and Nuclear Engineering, 30 Reactorului Street, Bucharest-Magurele, 077125 Romania

<sup>2</sup> Accent Pro 2000, s.r.l., Nerva Traian 1, K6, Apt 26, Bucharest, 031041 Romania

<sup>3</sup> The Institute for Advanced Energy Kyoto University, Uji, Kyoto 6110011, Japan

E-mail: [violeta.iancu@eli-np.ro](mailto:violeta.iancu@eli-np.ro)

**Abstract.** The Nuclear Physics oriented pillar of the pan-European Extreme Light Infrastructure (ELI-NP) will host an ultra-bright, energy tunable, and quasi-monochromatic gamma-ray beam system in the range of 0.2–19.5 MeV produced by laser-Compton backscattering technique. The applied research program envisioned at ELI-NP targets to use nuclear resonance fluorescence (NRF) and computed tomography to provide new opportunities for industry and society. High sensitivity NRF-based investigations can be successfully applied to safeguard applications and management of radioactive wastes as well as to uncharted fields like cultural heritage and medical imaging. Gamma-ray radioscopy and computed tomography performed at ELI-NP has the potential to achieve high resolution in industrial-sized objects provided the detection challenges introduced by the unique characteristics of the gamma beam are overcome. Here we discuss the foreseen industrial applications that will benefit from the high quality and unique characteristics of ELI-NP gamma beam and the challenges they present. We present the experimental setups proposed to be implemented for this goal, discuss their performance based on analytical calculations and numerical Monte-Carlo simulations, and comment about constraints imposed by the limitation of current scintillator detectors. Several gamma-beam monitoring devices based on scintillator detectors will also be discussed.

## 1. Introduction

The Extreme Light Infrastructure-Nuclear Physics (ELI-NP) facility under construction in Romania will host two state of the art systems, a high power laser system and a high brilliance gamma beam system [1]. The research program of ELI-NP focuses on laser and gamma driven nuclear physics as well as on applied research and development. A great variety of interdisciplinary scientific projects with societal and technological impact like industrial applications, medical applications and material applications are under development at ELI-NP[2, 3, 4, 5]. All the applications envisioned at ELI-NP exploit the unique features of the future laser and gamma beams to deliver new opportunities for society and industry.

The ELI-NP gamma beam is produced through Compton backscattering of laser light of an accelerated electron beam [6]. The laser light is delivered by two high power and high quality J-class lasers. The electron acceleration is based on a two-stage warm LINAC accelerator. The first stage of acceleration will deliver electrons of energies up to 300 MeV which will be deflected to a low energy interaction point generating gamma rays up to 3.5 MeV. The second stage will



Content from this work may be used under the terms of the [Creative Commons Attribution 3.0 licence](https://creativecommons.org/licenses/by/3.0/). Any further distribution of this work must maintain attribution to the author(s) and the title of the work, journal citation and DOI.

accelerate electrons up to 700 MeV, which will be deflected to a high energy interaction point to generate gamma rays up to 19.5 MeV. The main characteristics of the LCS gamma beam are presented in Table 1.

**Table 1.** Design characteristics of the ELI-NP LCS gamma beam [6].

Energy (MeV)	2.0	3.45	9.87	19.5
Nr of photons/pulse within FWHM	$1.2 \cdot 10^5$	$1.1 \cdot 10^5$	$2.6 \cdot 10^5$	$2.5 \cdot 10^5$
Nr of photons/s within FWHM	$4.0 \cdot 10^8$	$3.7 \cdot 10^8$	$8.3 \cdot 10^8$	$8.1 \cdot 10^8$
Source rms size ( $\mu m$ )	12	11	11	10
Source rms divergence ( $\mu rad$ )	140	100	50	40
Macro repetition rate (Hz)	100	100	100	100
Nr of pulses per macropulse	32	32	32	32
Pulse to pulse separation (ns)	16	16	16	16
Pulse length rms (ps)	0.92	0.91	0.95	0.90

As a result of the electron beam structure and the laser recirculation time the photons are emitted in very high intensity and in short pulses [6]. The macropulse repetition rate is 100 Hz. Each macropulse consists of 32 pulses separated by 16 ns; each pulse is 1 ps long. The number of photons within a pulse is around  $10^5$ , which build up to  $10^8$  photons per seconds. The high intensity of the gamma beam constitutes a great opportunity for research and industry but also challenges for the current detection technology.

The gamma beam industrial applications that we envision are mainly nondestructive inspections of objects, which are grouped in active interrogations based on nuclear resonance fluorescence (NRF) and gamma ray radioscopy and computed tomography (CT). Here we describe the experimental setups under construction at ELI-NP, discuss their future performance based on analytical calculations and numerical simulations and comment on the challenges they present. In addition we present several gamma beam monitoring instruments based on scintillators that will determine the operational conditions and characterize the gamma beam.

## 2. NRF-based applications

Nuclear resonance fluorescence, a nuclear process that yields characteristic signatures for every nuclei, became an attractive method to use for non-destructive material composition studies and has already been tested in fields related to safeguards and waste management [7, 8, 9]. Prospective uses of NRF for uncharted fields like cultural heritage and medical diagnostics have been proposed and are yet to be demonstrated [10].

The setups dedicated to NRF-based applications to be developed at ELI-NP employ both the scattering and the transmission methods [2] and rely on the availability of a high-efficiency detector array. The ELI-NP array of detectors (ELIADE) will consist of eight segmented clover detectors and four LaBr<sub>3</sub> detectors placed on two rings at 90° and 135°. ELIADE is designed to measure gamma rays for the entire gamma-beam energy range and is optimized for high signal to background ratio [11]. The NRF transmission setup is sketched in Fig. 1. Here, ELIADE is placed downstream of the investigated object and measures the scattering of the transmitted beam of a witness foil, which is an enriched sample of the material of interest. A decrease in the NRF signatures detected at the resonance energy is correlated with the presence of a particular isotope in the object. A detector placed in the beam, downstream of the witness foil, measures the transmitted radiation.

Estimates of the NRF count rates for both the scattering and the transmission methods at ELI-NP suggest an improvement of around three orders of magnitude at ELI-NP compared to the available gamma-ray facilities [2]. A simulation study based on the NRF transmission method was carried out to obtain the transmission factor of the  $\gamma$ -rays of 2176 keV (excitation energy of  $^{238}\text{U}$ ) through an object that contains both  $^{235}\text{U}$  and  $^{238}\text{U}$  [12]. A clear distinction between the  $^{235}\text{U}$  and  $^{238}\text{U}$  distributions in the investigated object was made when the transmission factor of on-resonance  $\gamma$ -rays normalized by that of off-resonance  $\gamma$ -rays is used for the CT image reconstruction. Thus, NRF used in combination with computed tomography at ELI-NP can produce isotope-specific maps at single resonance level.

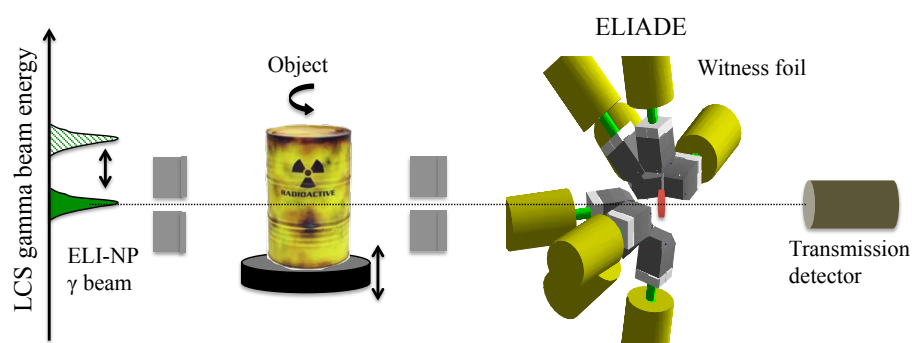


**Figure 1.** Schematic drawing of the transmission NRF setup

### 3. Radioscopy and computed tomography with brilliant gamma beams

Industrial gamma radioscopy and computed tomography using laser-Compton scattering (LCS) gamma beams have seen an increased interest lately because of the attractive characteristics of LCS beams as quasi monoenergetic, high intensity and high energy gamma beams [13]. It can be anticipated that these applications will benefit greatly from the unique characteristics of the ELI-NP LCS gamma beam [2]. The high-energy, high-intensity and narrow bandwidth ( $<0.5\%$ ) features of the gamma beam will allow investigation of large industrial objects with unprecedented resolution and practically free of beam hardening.

The setup that will be implemented at ELI-NP will specialize in non-destructive testing and analysis of various size objects by producing 2D transmission images and/or 3D reconstructed tomographs to reveal their internal fine structure and composition. These non-destructive analyses can be used to test the quality of industrial objects, e.g. inspect sinterizations, weldings or cracks in large objects. Two experimental configurations are under preparation: a pencil-beam and a cone-beam configuration. The pencil-beam configuration is sketched in Fig. 2. A high volume detector will absorb almost entirely the transmitted pencil beam while an automated positioning system capable of biaxial translation and rotation will be available for placing objects (up to 150 Kg) with high accuracy in beam. For cone-beam CT the high-volume detector will be replaced with a 2D gamma-ray imaging system.

An estimate on the performance of these setups was obtained using analytical methods and numerical simulations in GEANT4 [14, 15]. We estimated analytically the contrast of a stainless steel (SS) grid (see Fig. 2) against the background provided by homogeneous objects of various composition and in different configurations (see Ref. [2] for more details). For example, table 2 lists the expected thickness of several materials for which a contrast corresponding to 0.7 mm SS can be obtained in a single exposure of one second. Lots of exposures (as exemplified below) are needed to produce a radiograph or a CT image hence exposure times as small as possible are desired. The values listed in the table are produced using a source-object distance of 20

m, a magnification factor of 2, a detector efficiency of one and the gamma source intensity and divergence listed in Table 1. For instance, at 3.5 MeV one can obtain a contrast of 1.9 % in Al objects up to 40 cm in size and the same contrast in 13 cm of Fe block. The thickness doubles and almost triples at 9.87 and 19.5 MeV, respectively, thanks to the improved parameters of the gamma beam at high energy.

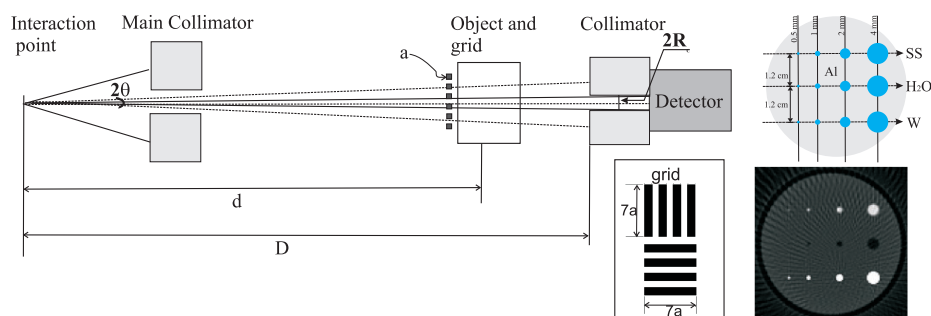


**Figure 2.** (a) Schematic drawing of the experimental setup and of the grid used to assess the resolution. A 2D CT image of phantom obtained from simulated data is shown on the right.

To test the spatial resolution and the contrast sensitivity of the tomography setup we have simulated the transmission through various objects and grids using Monte Carlo simulations implemented in GEANT4. We confirmed that photons scattered inside the object don't reach the detector and that images are free of beam hardening. Fig. 2 presents an example of a simulated 2D cross-sectional CT image of a phantom using the phantom composition shown in the same figure. The 2D cross-sectional image was obtained using filtered back-projection algorithm from 60 projections (3 degrees projection angle) with 109 views per projection (0.5 mm step). Each exposure was produced using a beam of  $1 \times 10^6$  photons/s of  $3.5 \text{ MeV} \pm 17 \text{ keV}$  and 0.5 mm beam spot [16]. Sub-millimeter (0.5 mm) features are best visible for high-density materials (higher contrast). In order to discriminate lower contrast parts (thin and low density objects) a smaller beam spot is desirable, which implies further collimation. Note that a smaller beam spot ( $< 0.5 \text{ mm}$ ) imply greatly reduced beam intensity for any conventional gamma source but not for the future gamma beam at ELI-NP, which is inherently narrow (divergence between  $200 \mu\text{rad}$  and  $40 \mu\text{rad}$ , see Ref. [6]) and the perfect solution for high-resolution tomography.

**Table 2.** Estimated thickness of given materials that can be scanned with 0.7 mm resolution.

Energy (MeV)	2	3.5	9.87	19.5
Al (cm)	30	41.2	88.9	104.9
Fe (cm)	10.4	13.5	23.7	24.3
H <sub>2</sub> O (cm)	70.8	100.5	250.1	337.05
Concrete (cm)	33.8	47	106.8	131.6
Photons/macropulse	$1.9 \times 10^3$	$2.9 \times 10^3$	$3.9 \times 10^3$	$3.4 \times 10^3$

While the performance of the radioscopy and computed tomography setup rely on the unique characteristics of the gamma beam it depends greatly on the detector performance. Table 2 lists also the number of photons per macropulse that a detector experiences for applications that

require high resolution and short exposure time for a pencil-beam setup. These values represent the number of photons that arrive at the detector in 32 bunches of picosecond duration separated by 16 ns. To cope with such high instant rates the detector has to be fast and radiation hard. The available scintillator detectors in use nowadays for tomography experiments have to be used with caution at ELI-NP because accidental absorption of full uncollimated beam can lead to radiation damage in the scintillator and high peak currents that will exceed the maximum values accepted for the photomultipliers (PMT). A search for alternative detection schemes for pencil-beam tomography is underway.

#### 4. Scintillator based gamma beam diagnostics instruments

The gamma beam produced at ELI-NP has unprecedented characteristics which call for constant monitoring and adjustment of its parameters to ensure proper operation. Most of the nuclear physics experiments and the applications described above require continuous and precise knowledge of the operational conditions, such as the beam energy and energy spread, beam intensity, the degree of polarization, the temporal structure and the spatial position.

Monitoring the parameters of the gamma-ray beam demands instruments capable of operating in radiation harsh environments, with fast response and excellent energy resolution. Several instruments based on scintillator materials have been proposed for this task because of their fast response time. An intensity and polarization monitor based on Li-glass and NE213-type detectors is proposed to measure the outgoing neutrons from the  $d(\gamma,n)p$  reaction [17, 18]. The gamma beam energy spread above 10 MeV will be monitored using a large volume  $\text{LaBr}_3$  detector with a  $\text{NaI(Tl)}$  anti-Compton shield placed in the attenuated beam [17]. Several additional instruments based on  $\text{LaBr}_3$  detectors are using Compton scattering and NRF for measuring the time structure, the intensity, and the polarization of the beam [17]. A thin  $\text{LYSO}$  scintillator sheet is foreseen to be placed in the gamma beam and in conjunction with a CCD camera would give insight into the spatial position of the beam and allow quick experimental instrument alignment.

The measurement of the beam intensity and polarization at energies above 3 MeV will take advantage of the large cross section and polarization asymmetry inherent in the  $d(\gamma,n)p$  reaction. The number of emitted neutrons peaks in the plane of beam polarization, and relatively few neutrons are emitted perpendicular to the plane of beam polarization. The neutron detectors should be oriented as shown in Fig. 3. The detector located at  $45^\circ$  with respect to the plane of beam polarization will be used to measure any misalignment in the plane of beam polarization or any component of circular polarization. This technique has been tested successfully at the HI $\gamma$ S facility [18].

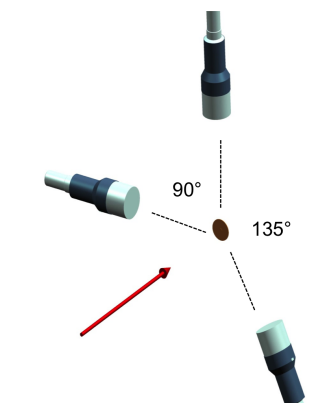


**Figure 3.** A schematic view of the relative position of the detectors for the polarization and intensity monitoring using either the NRF and the  $d(\gamma,n)p$  reaction. The beam is indicated by the red arrow, and the target is shown as a yellow disk.

The choice of neutron detector for the  $d(\gamma,n)p$  setup depends on the beam energy. For beam energies below 4 MeV, Li-glass detectors will be used to detect the outgoing neutrons. These



detectors can count with greater efficiency the 200–900 keV neutrons and are not subject to the same threshold effects as the liquid scintillator neutron detectors. For beam energies above 4 MeV, liquid scintillator neutron detectors based on EJ-309 scintillation material will be used. The advantages of using EJ-309 are its detection efficiency, which has been thoroughly studied, and its good pulse shape discrimination (PSD) properties. Moreover, the EJ309 detectors may be able to resolve nearby pulses since their short component decay time is around 4 ns. A conservative count rate estimate of 2 counts per macropulse, or 200 Hz, would allow for a measurement of the beam polarization to a statistical precision of 1% within a few minutes.

For time structure measurement,  $\text{LaBr}_3(\text{Ce})$ , with its 16 ns 1/e decay time, is indeed a very promising option for resolving individual pulses. Unfortunately, the rise and fall times increase with increasing crystal size, an effect arising from the increasing path length of scintillation photons in larger crystals. This effect is amplified by the difference in refractive index between  $\text{LaBr}_3$  and the boro-silicate glass used in the PMT windows, so that scintillation photons undergo many reflections before absorption at the photocathode. Tests at HI $\gamma$ S facility with a 16 ns time structure similar to the one developed at ELI-NP, demonstrate that a one inch detector is capable of reaching the anticipated decay time of 16 ns and the resulting spectra can be deconvoluted.

## 5. Conclusions

The gamma beam system at ELI-NP will deliver a very intense, quasi-monoenergetic and energy tunable gamma beam. This will be a perfect solution for industrial tomography applications as corroborated by our estimations based on analytical calculations and numerical simulations. The non-destructive assay of bulk materials based on NRF of can be successfully applied at ELI-NP thanks to the high-intensity gamma source and the high efficiency detector array. Scintillator based instruments are proposed for monitoring the characteristics of the gamma beam.

## Acknowledgments

The author(s) would like to acknowledge the help received from the engineering bureau, especially from Cristian Petcu and Emil Udup. The ELI-NP project is co-financed by the Romanian Government and European Union through the European Regional Development Fund.

## References

- [1] Zamfir N V 2016, *EPJ Web of Conferences* **117** 01001
- [2] Suliman G, Iancu V, Ur C A, Iovea M, Daito I, Ohgaki H 2016 *Rom. Rep. Phys* **68** S799
- [3] Bobeica M *et al.* 2016 *Rom. Rep. Phys* **68** S847
- [4] Asavei T *et al.* 2016 *Rom. Rep. Phys* **68** S275
- [5] Djourellov N, Hugenschmidt C, Balascuta S, Leca V, Oprisa A, Piochacz C, Teodorescu C and Ur C A 2016 *Rom. Rep. Phys* **68** S735
- [6] Adriani O *et al.*, 2014 Technical Design Report EuroGammaS proposal for the ELI-NP Gamma beam System, *Preprint* arXiv:1407.3669
- [7] Ludewigt B A, Quiter B J and Ambers S D 2011 *Nuclear resonance fluorescence for safeguards applications* (DOE report, url: <http://dx.doi.org/10.2172/1022713>.)
- [8] Bertozzi W and Ledoux R J 2005 *Nucl. Instr. and Meth. Phys. Res. B* **241**, 820
- [9] Toyokawa H *et al.* 2011 *Jap. J. of Appl. Phys.* **50** 100209
- [10] Lakshmanan M N, Harrawood B P, Agasthya G A, Kapadia A J 2014 *IEEE Trans. On Med. Imag.* **33** 546
- [11] Ur C A *et al.* 2016 *Rom. Rep. Phys* **68** S483
- [12] Daito I, Ohgaki H, Suliman G, Iancu V, Ur C A and Iovea M 2016 *Energy Procedia* **89** 389
- [13] Toyokawa H, Ohgaki H, Mikado T, and Yamada K 2002 *Rev. of Sci. Instrum.* **73** 3358
- [14] Agostinelli S *et al.* 2003 *J. Nucl. Instr. Meth. Phys. Res. A* **506** 250
- [15] Allison J *et al.*, 2006 *IEEE Trans. Nucl. Sci.* **53** 270
- [16] Suliman G, Iancu V, Ur C A, Iovea M, Daito I, Ohgaki 2016 *Int. J. of Modern Physics: Conference Series* **44** 1660216
- [17] Weller H R *et al.* 2016 *Rom. Rep. in Phys.* **68** S447
- [18] Matei C, Mueller J M, Sikora M H, Suliman G, Ur C A and Weller H R 2016 *J. of Instrum* **11** P05025